Archives of Materials Science and Engineering

Volume 105
Issue 2
October 2020
Pages 56-64

International Scientific Journal
published monthly by the
World Academy of Materials
and Manufacturing Engineering

DOI: 10.5604/01.3001.0014.5762

Simplified analyses of stress induced anisotropy in remolded soft clay under undrained conditions

P. Lin [a], Z.-x. Li [a], A. Garg [a], J.S. Yadav [b,*]

[a] Department of Civil and Environmental Engineering, Shantou University, China
[b] Department of Civil Engineering, National Institute of Technology Hamirpur, Hamirpur, India
* Corresponding e-mail address: jitendershine@gmail.com
ORCID identifier: https://orcid.org/0000-0001-6283-1588 (J.S.Y.)

ABSTRACT

Purpose: The soil's anisotropy induced by stress (i.e. stress induced anisotropy) has an important effect on the behavior of soil. This paper focuses on analyzing the anisotropy of remolded Shantou soft clay under compression stress path.

Design/methodology/approach: Experiments were executed by using three axle experimental instruments. The data obtained from the plain strain tests were analyzed and the relationship between stress and strain was calculated by using the modified Duncan-Chang and Lade-Duncan models. The models were modified under the condition of plain strain and cohesion.

Findings: It was concluded that in complex stress path conditions, the conventional triaxial tests may not fully reflect the actual stress of soil and its response in the Duncan-Chang and Lade-Duncan models.

Research limitations/implications: The formulation of Mohr-Coulomb failure criterion in the plasticity framework is quite diffcult. As a result, dilatancy cannot be described. The properties of soil in unload or drained conditions remain to be part of further investigated.

Practical implications: Based upon the two stiffness parameters, the modified Duncan-Chang model has captured the soil behaviour in a very conformable way and is recommened for practical modeling. These constitutive models of soil are widely used in the numerical analyses of soil structure such as embankments.

Originality/value: Duncan-Chang and Lade-Duncan models widely used in engineering practices are modes based on conventional triaxial cases. Both models have have some inherent limitations to represent the stress-strain characteristics of soils, such as shear-induced dilatancy and stress path dependency and required corrections. In this investigation, the tests are carried out in undrained conditions. It is related to the properties of soil in load conditions.

Keywords: Stress induced anisotropy, Shantou soft clay, True triaxial experiment

Reference to this paper should be given in the following way:

P. Lin, Z.-x. Li, A. Garg, J.S. Yadav, Simplified analyses of stress induced anisotropy in remolded soft clay under undrained conditions, Archives of Materials Science and Engineering 105/2 (2020) 56-64. DOI: https://doi.org/10.5604/01.3001.0014.5762

METHODOLOGY OF RESEARCH, ANALYSIS AND MODELLING

1. Introduction

Anisotropy induced by stress is a characteristic of soft clay which is different from the inherent anisotropy. Especially, it refers to the changes of physical properties and parameters on all directions as a result of different stress states under complex stress conditions [1]. When study is made on the stress induced anisotropy in the true triaxial experiment, it is necessary to eliminate all influencing factors, such as the effect of consolidation pressure (the difference between anisotropic consolidation and isotropic consolidation) [2,3]. The earliest study on anisotropy of soft clay starts in the study on transverse anisotropy. Wang et al. [4] conducted a series of tests on soft clay consolidated under different initial major principle stress direction. Torsional stress–strain relationships were found to be influenced by number of cycles. Strain components of soft clay including pore water pressure were affected by both Initial major principle stress direction and also intermediate principal stress coefficient. Qian et al. [5] studied effects of principal stress rotation using hollow cylindrical apparatus on stress-strain relationship of saturated soft clay. Similarly, Chen et al. [6] also observed anisotropy under rotational stresses. It identifies undrained failure, that results from growth of shear stresses as well as post-peak strength decay for Chicago and Boston blue clay. Xiao et al. [7] studied the hyper elasticity for granular medium in inherent and stress-induced anisotropy conditions by using a fabric tensor coupled with elastic potential energy density in terms of the elastic strain invariants. They concluded that such an approach provides unified considerations on the stress-induced and inherent anisotropic behaviour of the nonlinear elasticity and its stability. Wang et al. [8] performed a series of tests on natural K0-consolidated Wenzhou soft clay in a hollow cylinder apparatus to clarify the response of soils during principal stress rotation. During orientational shearing, the development of strain components (vertical, radial, circumferential, and shear strains) was clearly distinct. The coupling action of the axial and shear stresses resulted in different evolution processes of the excess pore-water pressure in tests with different β values [8]. Ling et al [9] conducted finite-element simulations to examine the capability of an anisotropic bounding surface model in simulating ground response due to deep excavations. The obtained simulation results were compared with published field measurements and with those obtained using the anisotropic Sekiguchi-Ohta and MIT-E3 models. They observed satisfactory agreement between finite-element simulations and field measurements in terms of lateral wall deflections and ground surface settlements. Wang et al. [10] conducted a series of drained tests on hollow cylinder apparatus to measure the anisotropy affected by β and b in natural soft marine clay. They provided the guidance for engineering projects in the coastal zone in terms of friction angle and deviator stress ratio with different b and β. Yin et al. [11] studied the anisotropic elastic–viscoplastic model for soft clays extended from overstress theory of Perzyna. The constant strain-rate oedometer test and the 24 h standard oedometer test were clayey carried out on soft clays and the parameters determined from these tests were examined. They reported that elastic–viscoplastic model can successfully reproduce the anisotropic and viscous behaviors of natural soft clays under different loading conditions. David and Rott [12] assessed the very small strain stiffness anisotropy of sedimentary clays. They reported that virgin oedometric loading of reconstituted clays leads to a development of inherent stiffness anisotropy, which cannot be easily reduced by subsequent loading.

Duncan [13] found in an undrained test that soft clay was differently strong in every direction, regardless of the over consolidation ratio of the sample. The vertical strength is greater than that in the horizontal direction. Strictly speaking, all undisturbed soil may be classified into the inherent anisotropy, with varying properties in the vertical and horizontal directions. Analysis of existing data and test results showed that undisturbed soil is a kind of horizontally anisotropic material. It means that when analyzing the undisturbed soil, one may analyze its properties in terms of horizontal anisotropy. In practice, it can also meet practical demands of engineering projects. Toyota et al. [14] evaluated the effects of stress induced anisotropy on the mechanical properties of saturated and unsaturated cohesive soils under different drainage conditions. They observed change of excess pore water pressure and suction during shearing generated strength anisotropy.

However, secondary anisotropy is the inconsistent characteristics in different directions as a result of the complex stress state of soil. The stress-strain law of soil sample greatly varies in different directions under different stress states. In many civil engineering practices, the presence of stress induces occurrence of anisotropy of the soil, such as dam impounding, basement construction, foundation pit excavation, etc., all of which are subject to anisotropy due to the change of stress state of the soil. Anisotropy of clay is important for design of geotechnical infrastructures [1]. The undrained loading is an essential factor in the stability and design of underground geotechnical infrastructures. The undrained shear strength is, however, not constant and may vary depending on rate, duration and direction of loading (anisotropy). Anisotropy of soft clay has proven to be important in ground movements induced by excavations [15]. Study on the secondary anisotropy of the soil helps to address practical engineering issues and furthers the understanding and application of the nature of soil.

In this investigation the soil samples were subjected to a series of plain strain test and constant middle principal stress ratio "*b*" test at different stress paths. The data obtained from the plain strain tests were analyzed and the relationship between stress and strain was calculated by using the modified Duncan-Chang and Lade-Duncan models. Modified Duncan-Chang model is widely used as its soil parameters can be easily obtained directly from standard triaxial test. It is a simple yet obvious enhancement to the Mohr-Coulomb model [26].

2. Soil used

This study adopts clay samples from Yashili Center Project, located at west section at entrance to Shantou Port, Shantou, China. The soil sample used in this study consists of 89.5% clay and 10.5% silt particle as shown in Figure 1. Its liquid limit and plastic limit are 36% and 25%, respectively. The predominant minerals present in clayey soil are kaolinite (52%), illite (18%), chlorite (20%) and other (10%). The basic physical and mechanical properties of the soil for the test as obtained by routine tests in the lab are shown in Table 1. The remoulded soft clay is in the absence of the inherent anisotropy compared to the undisturbed soil. In this study, the effect of the inherent anisotropy can be excluded.

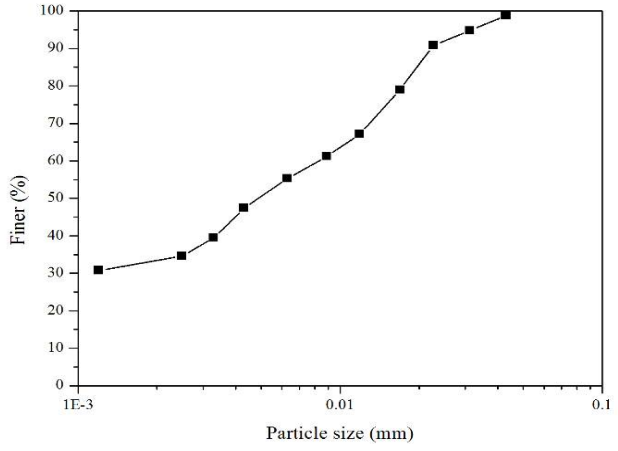

Fig. 1. Particle Size distribution curve of soil used

3. Test procedures

The ZSY-1 true triaxial loading device that provides mixed boundary conditions for a true triaxial apparatus was used in this study to simulate the stress paths of the soil. Experimental procedures adopted by Wang et al. [5,10] and Sawicki [16] was adopted.

In this investigation, the the natural clay specimens were trimmed by the specialized tool and specimens of 70 mm*35 mm*70 mm were prepared and tested. The specimens were enclosed in a rubber membrane and were placed in a large size chamber filled with water. The major principal stress (σ_1) and minor principal stress (σ_3) was applied to the specimens through test cell and top and bottom rigid caps as used in conventional triaxial apparatus. The intermediate principal stress (σ_2) was applied through horizontal loading system. The horizontal loading device consisted to two interconnected vertical plates that were located on opposite sides of the cubical specimen. On one laminated (alternate layers of stainless steel and balsa wood) horizontal plate, horizontal load was applied through pressure cylinder. The horizontal loading laminate plates were loaded by four ''legs'' fastened to the vertical loading rods. A load cell was placed directly on the top cap but below the ''leg'' fastening point to measure the vertical load directly on the specimen, to ensure that the vertical reaction force due to the laminate plates was not included. A small gap of 1 mm was left between the top (or bottom) cap and the laminate plates to avoid friction [17]. However, this gap causes inhomogeneous stress and strain during the test, leading to a decrease of the peak strength and an abnormal failure pattern [27]. The vertical and horizontal electro-mechanical actuators operate dynamically at frequencies up to 5 Hz. The maximum cell pressure was 2000 kPa. All the specimens were saturated at a back pressure of 300 kPa with an effective mean pressure of 20 kPa, followed by measuring the Skempton's B-value greater than 0.98. After that, the test specimens were isotropically consolidated under an effective confining pressure of 150 kPa. Similarly procedure was adopted by Kirkgard and lade [18] and Wang et al. [10] for determination of the anisotropy of noramlly consolidated bay mud and anisotropic drained deformation behavior and shear strength of natural soft marine clay, respectively.

Table 1.
The Physical and mechanical property parameters

Cohesion	Internal friction angle	Water content	Liquidity index	Plasticity index	Unit weight	Porosity	Modulus in Compression [28]
c, kPa	Φ, °	w, %	I_L	I_P	γ, kN/m^3	η	E, kPa
16.9	5.8	56	2.81	11	1.6	1.3	2.5

In this investigation the soil samples were subjected to a series of plain strain test and constant middle principal stress ratio "*b*" test at different stress paths. Plain strain exists in many engineering applications, such as embankment. In the plain strain test, the soil sample is undrained and consolidated to an appropriate state at constant confining pressure. It then receives the middle principal stress σ_2 load test at the same confining pressure. However, the constant middle principal stress ratio test may take the effect of middle principal stress on the sample into full account [19].

As to the elastic stage where normal consolidated soil was used, normal consolidated soil and low over-consolidated soil with the presence of low stress as proposed by Wheeler et al. [20] were always broken by plastic deformation. It may be essentially taken as anisotropy to simplify the elastic strain. In this experiment, the practical stress-strain relationship graph shows that the soil elastically changes in the stage under which elasticity is not developed. The sample was consolidated in an isotropic manner before the test. The constant ε_2 had a different direction during the test. Strain in the direction was maintained at zero. The consolidated undrained test was conducted, with the details are shown in Tables 2 and 3.

Table 2.
Plan of plain strain test

Test condition	Consolidation and test confining pressure, kPa		
σ_1 increase, σ_3 not changed	100	125	150

Note: the shear rate is 0.08 mm/min [21]

Table 3.
The constant middle principle stress test

Confining pressure, kPa	100	150	175
b value	0.3	0.5	0.75

Note: the shear rate is 0.08 mm/min

4. Test results

The relationship between pore water pressure and strain, deviator stress and strain at 100 kPa, 125 kPa, and 150 kPa confining pressure is shown in Figure 2. Pore water pressure under plain strain conditions increases with the increasing pressure, which is similar to the case in the conventional triaxial test, as shown in Figure 2. It is also the same case at different confining pressure as the one in conventional triaxial tests. However, in plain strain conditions, the limits to soil in the middle principal stress direction result in the effect on the development of pore water pressure.

As the consolidation pressure increases, the strength at failure of the soil also gradually rises, as shown in Figure 2. At 150 kPa, stress-strain presents an approximate straight line after going beyond the peak at different consolidation confining pressure, which represents the strength hardening property. Pore water pressure shares the same increase tendency as stress difference.

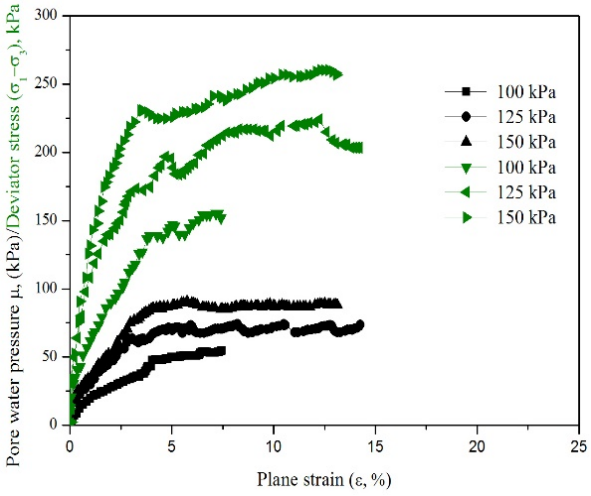

Fig. 2. Pore water pressure/deviator stress relationship with strain

The results of constant middle principal stress ratio test are shown in Figure 3. Figure 3 shows the $\varepsilon_1 - q$ relationship at confining pressure = 100 kPa. The initial tangent modulus of the soil sample increases as the middle principal stress ratio increases. With an increase of the ratio, the strain at time of sample failure decreases. It is much more obvious when compared to the failure strain at 15% of conventional triaxial case ($b = 0$). This indicates that the principal stress may reduce the failure strain of soil sample. Moreover, with the constraints of middle principal stress, the soil strength at failure is enhanced. Pore water pressure is the same as the deviatoric stress as the middle principal stress changes. The development of major principal strain is reduced significantly by an increasing cyclic intermediate principle stresses [22, 29].

In Figure 3 for $b = 0.75$, with initial strain stress increases rapidly while, for $b = 0.3$ and 0.5 initial stress is very low. Higher *b* value means more stiffness and it implies soil can sustain higher stresses at given strain with higher *b* value. Low *b* value means difference between cell pressure and pore pressure is very low initially and soil is less consolidated and hence may undergo higher strain. Comparison of development between pore water pressures at the same confining pressure finds that the middle principal stress has great effect on it. However, the deviatoric stress and strain curve shows that the soils retain its work hardening property at different middle principal stress ratios.

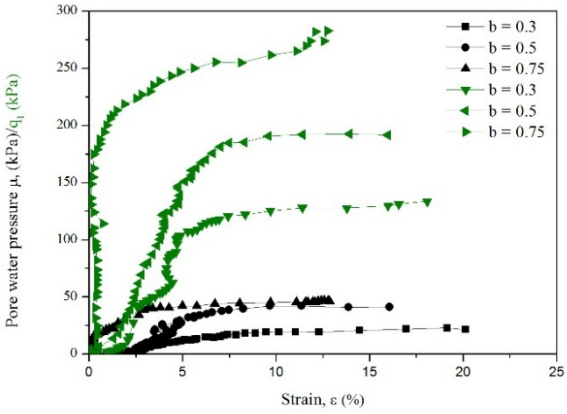

Fig. 3. $\varepsilon_1 - \mu$ / $\varepsilon_1 - q$ relationship with strain at confining pressure = 100 kPa

5. Analysis

These data show that the stress-strain relationship meet the property of strength hardening materials,whether in the plain strain stress or constant middle stress test. The plain strain test leads to the stress-strain relationship curve which is converted to the hyperbolic curve relationship graph $\frac{\varepsilon_1}{\sigma_1-\sigma_3} \approx \varepsilon_1$. The resulting curve approximates to a straight line. Therefore, it may be considered that Lade-Duncan elastic-plastic model and the variant can be used for checking the calculation [23].

Data processing

The hyperbolic curve relational expression $\frac{\varepsilon_1}{\sigma_1-\sigma_3} \approx \varepsilon_1$ and its curve obtained in the plain strain test are shown in the Figure 4. The relationship of $\log\frac{E_i}{P_a} \approx \log\frac{\sigma_a}{P_a}$ is shown in Figure 5. The elasticity parameters are tabulated in Table 4.

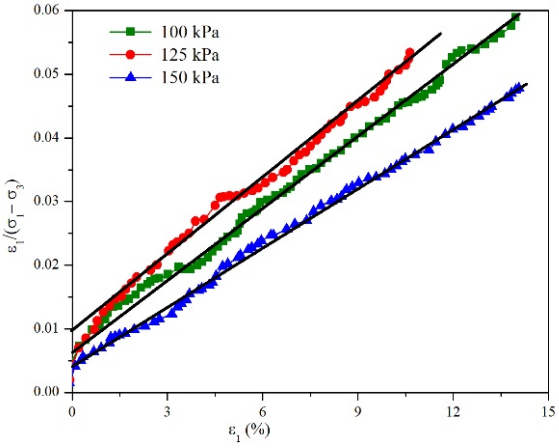

Fig. 4. $\frac{\varepsilon_1}{\sigma_1-\sigma_3} \approx \varepsilon_1$ relation

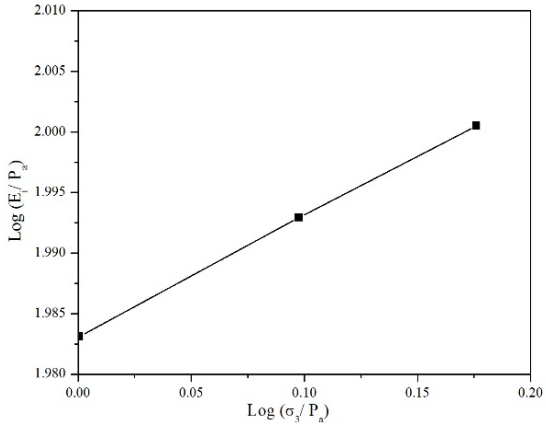

Fig. 5. Relationship of $\log\frac{E_i}{P_a} \approx \log\frac{\sigma_a}{P_a}$

Table 4.
The relationship between confining σ_3 and initial tangent modules E_i

σ_3, kPa	100	125	150
a	0.0058	0.0054	0.0033
E_i	9615.1	9846.1	10006.9

The approximation formula of initial tangent modulus for the stress-strain curve $E_i = kP_a\left(\frac{\sigma_3}{P_a}\right)^n$ is used, where n = 0.0988, k = 94. According to Bishop Relationship and stress increment relationship in plain strain state, it can be seen that Poisson's ratio at the plain strain is a constant. The Poisson's ratio μ of cohesive soil can be 0.35.

Determination of plasticity parameter

Lade-Duncan elastic-plastic model should be corrected to some extent if it is to be used in the clay plain strain test because Lade-Duncan elastic-plastic model is based on the triaxial test of non-cohesive soil. Qiang [23] and Ding [24] further extend Lade-Duncan to plain strain against the correction of Lade-Duncan model and based on the conclusion that is may be extended to the range of cohesive soil. The principal theory is to assume that the middle principal stress in the plain strain conditions.

$$\sigma_2 = \sqrt{\sigma_1\sigma_3} \tag{1}$$

Lade-Duncan is used as the basis for the fact that Lade-Duncan rule is applied to plain strain, and the bond stress σ_o is cited for its correction so that it is applicable to cohesive soil.

Then, according to the breaking rule of Lade-Duncan model:

$$F = \frac{(I_1)^3}{I_3} = \mathrm{K} \tag{2}$$

By substituting formula (1) into (2), there is:

$$\frac{\sigma_1}{\sigma_3} = R_{ps} = \frac{1}{4}\left[\sqrt[3]{K} - 1 + \sqrt{\left(\sqrt[3]{K} - 1\right)^2 - 4}\right]^2 \quad (3)$$

where: R_{ps} is the maximum/minimum principal stress ratio at failure under plain strain conditions. Assuming that $R_{ps} = \eta$, there is:

$$\sigma_1 = \eta\sigma_3$$

The stress expression following introduction of σ_o is:

$$\sigma_i = \overline{\sigma_i} + \sigma_o \text{ (i= 1, 2, 3)}$$

where: $\sigma_o = c_{\tau c}\cot\varphi_{\tau c}$. $c_{\tau c}$ is the cohesion force under the triaxial compression conditions.

The Laden-Duncan rule-based breaking rule of cohesive soil under the plain strain conditions is:

$$\overline{\sigma_1} - \eta\overline{\sigma_3} - (\eta - 1)\sigma_o = 0 \quad (4)$$

where: $\eta = \frac{1}{4}\left[\sqrt[3]{K} - 1 + \sqrt{\left(\sqrt[3]{K} - 1\right)^2 - 4}\right]^2$

$$K = \frac{(3 - \sin\varphi_{\tau c})^3}{(1 + \sin\varphi_{\tau c})(1 - \sin\varphi_{\tau c})^2}$$

The flow method uses uncorrelated flow rule. However, it is required that same form but different material parameters should be assumed for the potential plain and the loading plain of plasticity:

$$Q = \frac{l_1^3}{l_3} - k_1 = 0$$

or:

$$Q = l_1^3 - k_1 l_3 = 0$$

The hardening rule uses the law of plastic hardening work expressed as:

$$k_1 = H(W_p) = H\left(\int \sigma_{ij}\, d\varepsilon_{ij}^p\right)$$

The resulting plastic stress-strain relationship will be:

$$\begin{Bmatrix} d\varepsilon_1^p \\ d\varepsilon_2^p \\ d\varepsilon_3^p \end{Bmatrix} = d\lambda k_1 \begin{Bmatrix} \frac{3l_1^3}{k_1} - \sigma_2\sigma_3 \\ \frac{3l_1^3}{k_1} - \sigma_1\sigma_3 \\ \frac{3l_1^3}{k_1} - \sigma_1\sigma_2 \end{Bmatrix} \quad (5)$$

It can been seen in the formula above that solving the stress-strain relationship in (4) requires solutions to parameter k_i of the plastic potential and the plastic factor $d\lambda$. According to the definition of Poisson's ratio:

$$-\mu^p = \frac{d\varepsilon_3^p}{d\varepsilon_1^p} = \frac{3l_1^2 - k_1\sigma_1\sigma_2}{3l_1^2 - k_1\sigma_2\sigma_3}$$

The plastic parameter k_1 can be obtained:

$$k_1 = 3\frac{l_1^2(1+\mu^p)}{\sigma_3(\sigma_1+\sigma_3\mu^p)} \quad (6)$$

Therefore, the result of k_1 can be obtained from the experimental results as shown in Figure 6.

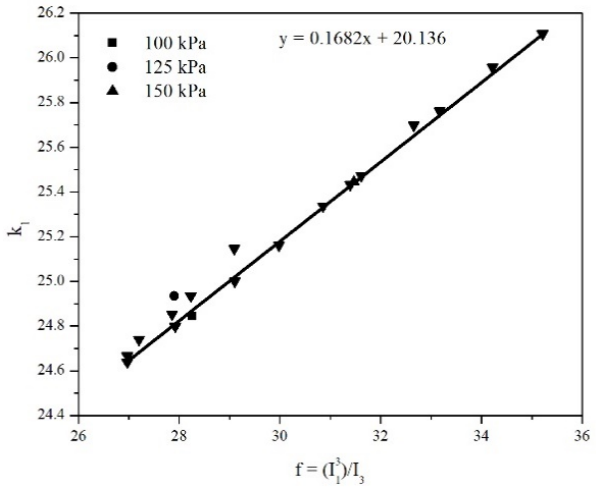

Fig. 6. Relationship of k_1 and f

The relationship curve between the plastic potential parameter k_1 and yield function shows a linear relationship. Because the principal stress in soil samples varies under plain strain, the curve of k_1-f derived from this condition is not affected by the ration of middle principal stress 'b'. The equation can be expressed as follows:

k_1=Af+B

where: A and B are test parameters

With the regression analysis, the plastic potential parameter k_1 may be expressed in:

k_1=0.168*f+20.13

On the other hand, plastic factor $d\lambda$ may be obtained according to the law of plastic work hardening $k_1 = H(W_p) = H\left(\int \sigma_{ij}\, d\varepsilon_{ij}^p\right)$ and the relationship between plastic work and stress level.

The plastic work is $W_p = \int \sigma_{ij}\, d\varepsilon_{ij}^p$,

So it can be obtained according to the law of plastic work hardening that:

$$dk = H'\left(pd\varepsilon_v^p + qd\varepsilon_s^p\right)$$

According to the flow rule and Euler cubic homogenous equation, it can be obtained that:

$$dk = H'd\lambda\left(p\frac{\partial Q}{\partial p} + q\frac{\partial Q}{\partial q}\right)$$

$$p\frac{\partial Q}{\partial p}+q\frac{\partial Q}{\partial q}=3Q$$

so: $d\mathrm{k}=3\mathrm{Q}\mathrm{H}'\mathrm{d}\lambda$

$$\begin{cases} d\lambda=\dfrac{dW_p}{3Q} \\ f-f_\tau=\dfrac{W_p}{a+bW_p} \end{cases}$$

According to both formulas above, there is:

$$dW_p=\frac{a}{[1-b(f-f_\tau)]^2}df$$

so: $$d\lambda=\frac{a}{3(l_1^3-k_1l_3)[1-b(f-f_\tau)]^2}df \tag{7}$$

where: *a, b* are curve parameters. It can be obtained from the experimental data that: f_τ is the initial stress level $f_\tau=l_1^3/l_3$. On isotropic consolidation, $l_1=3\sigma_3$, $l_3=3\sigma_3^3$, so there is $f_\tau=27$.

Figure 7 represents the relationship between plastic work and stress level at different consolidation confining pressures. Parameters a and b are obtained, as shown in Table 5. By substituting the resulting equations (5)-(6) of the plastic factor $d\lambda$ and the plastic potential parameter k_1 into equation (4), the plastic strain may be obtained.

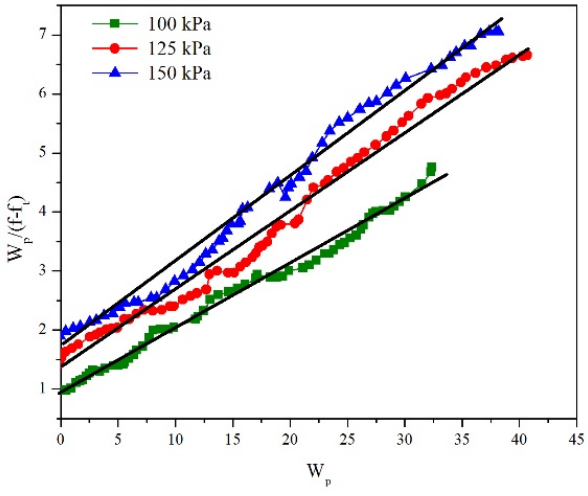

Fig. 7. Relationship of $W_p/(f\text{-}f_t)$ to W_p

Table 5.
Value of *a* and *b* at various σ_3

Confining pressure, kPa	100	125	150
a	0.981	1.245	1.57
b	0.107	0.139	0.15

By substituting the resulting equations (5)-(6) of the plastic factor $d\lambda$ and the plastic potential parameter k_1 into equation (4), the plastic strain may be obtained.

An elastic-plastic matrix or an elastic matrix is developed in the course of simulated loading. The variant or strain increment is calculated. The actual value is simulated, compared and fitted by the model at the elastic deformation stage or at low confining pressure of the soil.

6. Conclusions

Lade-Duncan model used in this paper is a simple shear yielding model. The true triaxial test is used for the consolidated undrained test of Shantou soft clay under plain strain conditions. Stress-strain relationship is analyzed at specific stress paths according to the test data and Lade-Duncan model. Lade-Duncan model is corrected by introducing cohesive soil and plain strain conditions so that it can be used within cohesive soil. It is analyzed that in complex stress path conditions, the conventional triaxial tests may not fully reflect the actual stress of soil and its response. Duncan-Chang and Lade-Duncan models widely used in engineering practices are modes based on conventional triaxial cases. Both models have have some inherent limitations to represent the stress-strain characteristics of soils, such as shear-induced dilatancy and stress path dependency and required corrections. In this investigation, the tests are carried out in undrained conditions. It is related to the properties of soil in load conditions. The properties of soil in unload or drained conditions remain to be further investigated.

Scope of future work

The modified Duncan-Chang model is preferred over the elastoplastic model used by Wheeler et al. [20] and Hong et al. [25]. Failure itself is described by means of the Mohr-Coulomb failure criterion, but this is not properly formulated in the plasticity framework [26]. As a result, dilatancy cannot be described. Based upon the two stiffness parameters, the modified Duncan-Chang model has captured the soil behaviour in a very conformable way and is recommened for practical modeling. These constitutive models of soil are widely used in the numerical analyses of soil structure such as embankments. Future investigation should be foucsed on utilization of model by Hong et al. [25] for analyzing behavior of cohesive soil under plain condition. More systematic studies are required comparing effects of different soil types and also under varying stress paths for understanding behaviour of soil. The detailed theoretical development is also required to capture the

antistrophic behaviour of various soils. Further improvement in theoretical models are required.

Notations

a, b	Skempton's Parameter
σ_1	Major principal stress, kPa
σ_2	Intermediate principal stress, kPa
σ_3	Minor principal stress, kPa
σ_o	Bond Stress, kPa
μ	Pore water pressure, kPa
ε	Strain, %
E_i	Initial Tangent modules, kPa
I_1	First stress invariant
I_3	Third stress invariant
R_{ps}	Maximum/Minimum principal stress ratio
$c_{\tau c}$	Cohesion force under the triaxial compression, kPa

Acknowledgements

The authors are highly thankful to the Department of Civil and Environmental Engineering, Shantou University for proving the necessary equipment for conducting this investigation.

References

[1] F.-C. Teng, C.-Y. Ou, P.-G. Hsieh, Measurements and numerical simulations of inherent stiffness anisotropy in soft Taipei clay, Journal of Geotechnical and Geoenvironmental Engineering 140/1 (2014) 237-250. DOI: https://doi.org/10.1061/(ASCE)GT.1943-5606.0001010

[2] N.M. Rodriguez, P.V. Lade, True triaxial tests on cross-anisotropic deposits of fine Nevada sand, International Journal of Geomechanics 13/6 (2013) 779-793. DOI: https://doi.org/10.1061/(ASCE)GM.1943-5622.0000282

[3] H. Toyota, A. Susami, S. Takada, Anisotropy of undrained shear strength induced by K 0 consolidation and swelling in cohesive soils, International Journal of Geomechanics 14/4 (2014) 04014019. DOI: https://doi.org/10.1061/(ASCE)GM.1943-5622.0000344

[4] Y. Wang, Y. Gao, B. Li, L. Guo, Y. Cai, A.H. Mahfouz, Influence of initial state and intermediate principal stress on undrained behavior of soft clay during pure principal stress rotation, Acta Geotechnica 14/5 (2019) 1379-1401. DOI: https://doi.org/10.1007/s11440-018-0735-5

[5] J.Qian, Z. Du, X. Lu, X. Gu, M. Huang, Effects of principal stress rotation on stress–strain behaviors of saturated clay under traffic–load–induced stress path, Soils and Foundations 59/1 (2019) 41-55. DOI: https://doi.org/10.1016/j.sandf.2018.08.014

[6] Y. Chen, F. Marinelli, G. Buscarnera, A rotational hardening model capturing undrained failure in anisotropic soft clays, Indian Geotechnical Journal 49/4 (2019) 369-380. DOI: https://doi.org/10.1007/s40098-018-0339-x

[7] Y. Xiao, Z. Zhang, J. Wang, Granular hyperelasticity with inherent and stress-induced anisotropy, Acta Geotechnica 15/3 (2020) 671-680. DOI: https://doi.org/10.1007/s11440-019-00768-z

[8] J. Wang, D. Feng, L. Guo, H. Fu, Y. Cai, T. Wu, L. Shi, Anisotropic and Noncoaxial Behavior of K 0-Consolidated Soft Clays under Stress Paths with Principal Stress Rotation, Journal of Geotechnical and Geoenvironmental Engineering 145/9 (2019) 04019036. DOI: https://doi.org/10.1061/(asce)gt.1943-5606.0002103

[9] H.I. Ling, C. Hung, V.N. Kaliakin, Application of an enhanced anisotropic bounding surface model in simulating deep excavations in clays, Journal of Geotechnical and Geoenvironmental Engineering 142/11 (2016) 04016065. DOI: https://doi.org/10.1061/(ASCE)GT.1943-5606.0001533

[10] Y.-K. Wang, L. Guo, Y.-F. Gao, Y. Qiu, X.-Q. Hu, Y. Zhang, Anisotropic drained deformation behavior and shear strength of natural soft marine clay, Marine Georesources & Geotechnology 34/5 (2016) 493-502. DOI: https://doi.org/10.1080/1064119X.2015.1081653

[11] Z.-Y. Yin, C.S. Chang, M. Karstunen, P.-Y. Hicher, An anisotropic elastic–viscoplastic model for soft clays, International Journal of Solids and Structures 47/5 (2010) 665-677. DOI: https://doi.org/10.1016/j.ijsolstr.2009.11.004

[12] D. Mašín, J. Rott, Small strain stiffness anisotropy of natural sedimentary clays: review and a model, Acta Geotechnica 9/2 (2014) 299-312. DOI: https://doi.org/10.1007/s11440-013-0271-2

[13] J.M. Duncan, Anisotropy and stress reorientation in clay, Journal of the Soil Mechanics and Foundations Division 92/5 (1966) 21-50.

[14] H. Toyota, S. Takada, A. Susami, Mechanical properties of saturated and unsaturated cohesive soils with stress-induced anisotropy, Géotechnique 68 (2017) 883-892. DOI: https://doi.org/10.1680/jgeot.17.p.018

[15] R.J. Finno, X. Tu, Selected topics in numerical simulation of supported excavations, Proceedings of the International Conference on Numerical Simulation of Construction Processes in Geotechnical Engineering for Urban Environment – Numerical Modelling of Construction Processes in Geotechnical Engineering for Urban Environment, Bochum, 2006, 3-19.

[16] A. Sawicki, J. Mierczyński, A. Mikos, J. Sławińska, Liquefaction resistance of a granular soil containing some admixtures of fines, Archives of Hydro-Engi-

neering and Environmental Mechanics 62/1-2 (2015) 53-64. DOI: https://doi.org/10.1515/heem-2015-0019
[17] J.H. Yien, C.M. Cheng, W.H. Kumruzzaman, New mixed boundary, true triaxial loading device for testing three-dimensional stress–strain–strength behavior of geomaterials, Canadian Geotechnical Journal 47/1 (2009) 1-15. DOI: https://doi.org/10.1139/T09-075
[18] M.M. Kirkgard, P.V. Lade, Anisotropic three-dimensional behavior of a normally consolidated clay, Canadian Geotechnical Journal 30/5 (1993) 848-858. DOI: https://doi.org/10.1139/t93-075
[19] Q. Wang, P.V. Lade, Shear banding in true triaxial tests and its effect on failure in sand, Journal of Engineering Mechanics 127/8 (2001) 754-761. DOI: https://doi.org/10.1061/(ASCE)0733-9399(2001)127:8(754)
[20] S.J. Wheeler, A. Näätänen, M. Karstunen, M. Lojander, An anisotropic elastoplastic model for soft clays, Canadian Geotechnical Journal 40/2 (2003) 403-418. DOI: https://doi.org/10.1139/t02-119
[21] T.M. Thu, H. Rahardjo, E.-C. Leong, Shear strength and pore-water pressure characteristics during constant water content triaxial tests, Journal of Geotechnical and Geoenvironmental Engineering 132/3 (2006) 411-419. DOI: https://doi.org/10.1061/(ASCE)1090-0241(2006)132:3(411)
[22] C. Gu, Y. Wang, Y. Cai, J. Wang, Deformation characteristics of saturated clay in three-dimensional cyclic stress state, Canadian Geotechnical Journal 56/12 (2019) 1789-1802. DOI: https://doi.org/10.1139/cgj-2018-0634
[23] Q. Jiang, J.-m. Zhu, Y.-p. Yao, Application of Lade-Duncan failure criterion to calculation of bearing capacity of foundation, Chinese Journal of Rock Mechanics and Engineering 24/18 (2005) 3262-3265.
[24] L. Ding, The plain strain strength formula of soil based on the SMP criterion. Journal of Geotechnical Mechanics (2000) 390-393.
[25] Y. Hong, L. Wang, J. Zhang, Z. Gao, 3D elastoplastic model for fine-grained gassy soil considering the gas-dependent yield surface shape and stress-dilatancy, Journal of Engineering Mechanics 146/5 (2020) 04020037. DOI: https://doi.org/10.1061/(ASCE)EM.1943-7889.0001760
[26] K.S. Ti, B.B.K. Huat, J. Noorzaei, M.S. Jaafar, G.S. Sew, A review of basic soil constitutive models for geotechnical application, Electronic Journal of Geotechnical Engineering 14 (2009) 1-18.
[27] Z. Li, L. Wang, Y. Lu, W. Li, K. Wang, H. Fan, Experimental investigation on true triaxial deformation and progressive damage behaviour of sandstone, Scientific Reports 9/1 (2019) 3386. DOI: https://doi.org/10.1038/s41598-019-39816-9
[28] Q. Yang, W.-M. Leng, S. Zhang, R.-S. Nie, Experimental Study on Compression Modulus of Sandy Soil, Proceedings of the 2nd International Conference Challenges and Recent Advances in Geotechnical and Seismic Research and Practices "IACGE 2013", Chengdu, China, 2013, 287-296. DOI: https://doi.org/10.1061/9780784413128.035
[29] C. Gu, Y. Wang, Y. Cui, Y. Cai, J. Wang, One-way cyclic behavior of saturated clay in 3D stress state, Journal of Geotechnical and Geoenvironmental Engineering 145/10 (2019) 04019077. DOI: https://doi.org/10.1061/(ASCE)GT.1943-5606.0002137